

Radiation pressure instability: from heart-beat states in black hole binary systems to Quasars and Changing-Look AGN

Agnieszka Janiuk,^{a,*} Bozena Czerny,^a Pulkit Ojha,^a Yuri Cavecchi^b and Federico Vincentelli^{c,d}

^aCenter for Theoretical Physics, Al. Lotnikow 32/46, 02-668, Warsaw, Poland

^bDepartament de Física, EEBE, Universitat Politècnica de Catalunya, Av. Eduard Maristany 16, 08019 Barcelona, Spain

^cFluid and Complex Systems Centre, Coventry University, CV1 5FB, UK

^dINAF—Istituto di Astrofisica e Planetologia Spaziali, Via del Fosso del Cavaliere 100, I-00133 Roma, Italy

E-mail: agnes@cft.edu.pl

Radiation-pressure instability was identified soon after the seminal classical accretion disk models of Shakura & Sunyaev and Novikov & Thorne, yet its full implications remain an active area of investigation. These models form the backbone of our understanding of accretion onto compact objects and successfully describe the phenomenology of black hole and neutron star X-ray binaries, as well as luminous active galactic nuclei (AGN), in the regime of high mass accretion rates. At luminosities approaching a significant fraction of the Eddington limit ($L/L_{\text{Edd}} \geq 0.1$), standard thin disks are predicted to become thermally unstable due to the dominance of radiation pressure. This prediction has found empirical support in several Galactic stellar-mass black hole systems, where the instability manifests as quasi-periodic, large-amplitude luminosity oscillations, so-called “heartbeat states”, and has been proposed as a driver of observed signatures of deterministic chaos in accretion-driven light curves.

The scope of radiation-pressure-induced variability extends beyond stellar-mass black holes: both black holes across mass scales and accreting neutron stars can exhibit related behavior, though the presence of a boundary layer in neutron stars adds complexity and offers a unique laboratory for testing the interplay between accretion dynamics and the central object. On extragalactic scales, the instability has been invoked to explain the duty cycles and apparent short lifetimes of radio-loud AGN, as well as the dramatic spectral-state transitions seen in Changing-Look AGN.

Despite these advances, the theoretical picture remains unclear. State-of-the-art magnetohydrodynamic (MHD) simulations have not yet reached consensus on the conditions under which the radiation-pressure instability fully develops or is suppressed. Magnetic fields, which mediate angular momentum transport and couple to both gas and radiation, emerge as a potentially critical factor in modulating the instability’s onset and nonlinear evolution. This lecture will revisit the historical development of the instability concept, survey the current observational and theoretical status across different classes of accreting compact objects, and highlight the key open questions in the theory and the connection to observed variability phenomenology, that will shape the next fifty years of disk instability research.

*Speaker

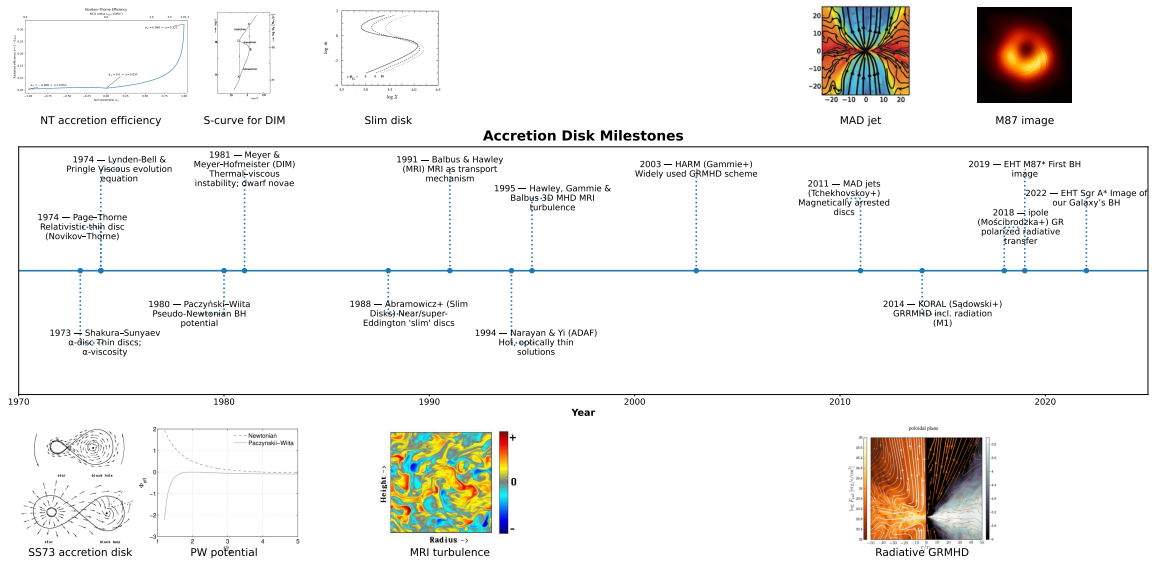


Figure 1: Schematic timeline showing milestones in the accretion theory

1. Introduction

Accretion disks are known to power the X-ray binaries with compact objects and AGN. The variability of observed emission encodes physical processes underlying the heating and cooling of the plasma and the transport of angular momentum that enables accretion. The stochastic type of variability is found in most states of various objects, across their mass scale. However, a distinct type of periodic, or quasi-periodic flares, is occasionally observed, pointing towards a deterministic nature of the process.

The physical mechanism behind such cyclic variations is the Radiation Pressure Instability (RPI). This instability produces regular outbursts, and flare-like events that represent low-dimensional chaos. It may also be responsible for the duty cycles in some objects and lead to an on-off behavior or intermittent activity. The physical nature of the RPI driven variability is connecting the micro- and macro-scales, because it is related to the stress tensor scaling with pressure in the plasma, and also to directly probe the viscosity magnitude and timescales of secular changes. Observational signatures of the RPI span from the heartbeat states observed in microquasars (tens-hundreds of seconds) to Quasars and Changing-Look AGN (tens -thousands of years).

2. Brief history of accretion disks

The theory of accretion disks was proposed to explain the appearance of high energy emitting sources related to white dwarfs, black holes or neutron stars residing in binary systems located in our Galaxy. These compact stars gain material from their companion stars in either high mass or low mass regime, where the companion star may fill its Roche lobe and donate material through the Lagrangian L_1 point, or via the focused stellar winds. N. Shakura and R. Sunyaev proposed in [28] that the material in both cases forms a geometrically thin, optically thick disk in the orbital plane of the binary system. In order to lose the angular momentum and proceed to lower orbits around the

accretor, the gas layers shear against each other and the angular momentum is transported outwards by viscosity. The turbulent nature of the process implies an effective scaling of viscous turbulent velocity and length-scale, with the speed of sound and disk vertical scale-height. A concurrent model proposed by Novikov & Thorne [20] proved the efficiency of the process leading to viscous energy dissipation being very large with respect to the rest-mass energy of accreting particles, and growing enormously with the black holes spin. Hence, accreting Kerr black holes are the most powerful sources of energy expected so far in the Universe.

In Figure 1, we present a timeline visualising the milestones achieved in the accretion disk theory. For completeness, the graph ends with some current state-of-the-art numerical models¹, which are not the scope of this Proceeding, but will be commented briefly in the last Section. In 1970's along with Shakura-Sunyaev model, Lynden-Bell & Pringle [19] showed that a thin Keplerian disc with an effective kinematic viscosity evolves diffusively. The viscosity causes angular momentum to flow outward and mass to flow inward. They derived the surface density diffusion equation with self-similar solutions, and for a viscosity that scales as a power of radius, their explicit similarity solutions describe how an initially ring-like mass distribution spreads over time. This work provides a general framework for the time-dependent evolution of viscous accretion discs.

The viscous and thermal instability mechanism that can potentially lead to the disk disruption, was identified by Lightman & Eardley [16] who showed that the standard Shakura–Sunyaev α -disk with stress proportional to the total pressure is unstable in the radiation-pressure-dominated inner region. The equilibrium branch of this solution exhibits (i) thermal instability, because the heating grows faster than cooling for a temperature perturbation, and (ii) viscous (secular) instability, because the effective diffusion coefficient becomes negative, since accretion rate decreases with increasing surface density. The thermal instability itself was then discussed in the context of two-temperature optically thin disks by [30]. These SLE disks are unstable because of thermal runaway: their heating rate grows faster than cooling rate, at fixed density (however, they are viscously stable).

A next milestone that boosted the first numerical works on accretion disks evolution, was the Paczynski-Wiita potential, introduced in [24]. It exactly reproduces the locations of the innermost stable circular orbit (ISCO) and the marginally bound orbit, and gives the correct functional form of the specific angular momentum distribution. Despite the mathematical simplicity, it captures key strong-gravity features of a Schwarzschild black hole. Therefore, while still working in a Newtonian hydrodynamics framework, it is widely used in analytic models and simulations of black-hole accretion disks when full GR is unnecessary or too expensive.

The disk instability (DIM) model proposed for outbursts driven by a thermal–viscous instability, is not a purely thermal one. The mechanism was discussed in [21] and [31]. They showed that locally, the instability is triggered when the disc temperature enters the hydrogen partial-ionization regime, because then the opacity and pressure respond very steeply to temperature, so a small heating makes heating rate rise faster than cooling. In an α -disc, the viscosity also depends strongly on temperature. Along the middle branch of the S-curve (visualised in the insert of Fig. 1) the solution is both thermally and viscously unstable, so the same physical mechanism gives thermal and

¹We mention Narayan-Yi ADAF model, the GR MHD numerical schemes, MAD disks and relativistic jets, and polarized radiation transport simulations as the milestones

secular (viscous) instability. This is producing the limit cycle between the cold and hot branches, commonly used to explain the outbursts of Dwarf Novae.²

The RPI instability is also of thermal-viscous type, as argued above. In order to produce an outburst cycle, some stabilizing mechanism must be found. It was possible only thanks to the slim disk model [1] who presented a new branch of stationary accretion-disk equilibria at $\dot{M} \sim \dot{M}_{\text{Edd}}$ around black holes. This branch closes the S-curve of RPI instability (cf. Fig. 1). It exists once the radial advection of heat in an optically thick, nearly Keplerian disk is properly included. These “slim disks” are geometrically thicker than standard thin disks but they are not as torus-like as the other famous solutions - Polish “doughnuts”, e.g [24]. A substantial fraction of the dissipated energy is advected inward rather than radiated locally, so their luminosity saturates and can only modestly exceed the Eddington value. The slim disks are quasi Keplerian, and keep the H/R ratio well below 1.

3. Physical origin of Radiation Pressure instability

In Fig. 2 we show the physical regions in the Shakura-Sunyaev α disks where either radiation pressure and electron scattering opacity dominates (blue region), or the gas pressure with electron scattering is dominant (orange region) or the gas pressure with Kramer’s opacity dominates (green region). The location of the zones depends on the accretion rate. The Eddington accretion rate for adopted compact object with mass $1.4M_{\odot}$ (black hole or neutron star) and accretion efficiency of $\eta = 0.1$ is marked with red horizontal line. The location of the radiation pressure dominated zone is plotted for assumed viscosity parameter $\alpha = 0.1$. In addition, the blue line marks the region where the disk midplane temperature in the disk drops below 10^4 K, so that other opacity sources than Kramers’ become important, due to hydrogen recombination. That region is unstable, according to the DIM model, until temperature drops below $\sim 3 \times 10^3$ K, when the hydrogen is fully neutral.

We notice that for WD, BH and NS, both regions of instabilities due to P_{rad} and Hydrogen partial-ionisation can exist in the same disk, if only the accretion rate is high and the disk size, limited by Roche lobe size, is also large enough. For WD, the radiation pressure zone is not extending beyond the WD radius, so in practice we will not observe this kind of instability.

Conceptually, in the plot of local thermal equilibria (see Fig. 3; at fixed radii), the inclusion of advection gives an extended S-curve. A lower Shakura–Sunyaev thin-disk branch, an intermediate (unstable) radiation-pressure region, and an upper, advective, slim-disk branch that is thermally and viscously stable. This is closely analogous in mathematical structure to the DIM S-curve for dwarf novae, even though the physical origin of the extra branches (radiation pressure + advection rather than H-ionization) is different.

The local equilibrium solutions are found by solving the heating and cooling balance. For slim disks, the relevant terms, describing the (vertically averaged) viscous heating and radiative plus

²Note that some reviews (e.g. Lasota 2001, Hameury 2009, 2019) explicitly trace the thermal–viscous DIM back to Hoshi (1979) for identification of the instability. The work of Osaki (1974) is also often cited as the first explicit accretion disk outburst model for dwarf novae (the seed of the DIM), while Hoshi (1979) provided the detailed thermal instability and bimodal-state disc structure (the S-curve). Also, Honma, Matsumoto, & Kato (1991) for the first time succeeded in producing repetitive bursts occurring due to the radiation pressure instability.

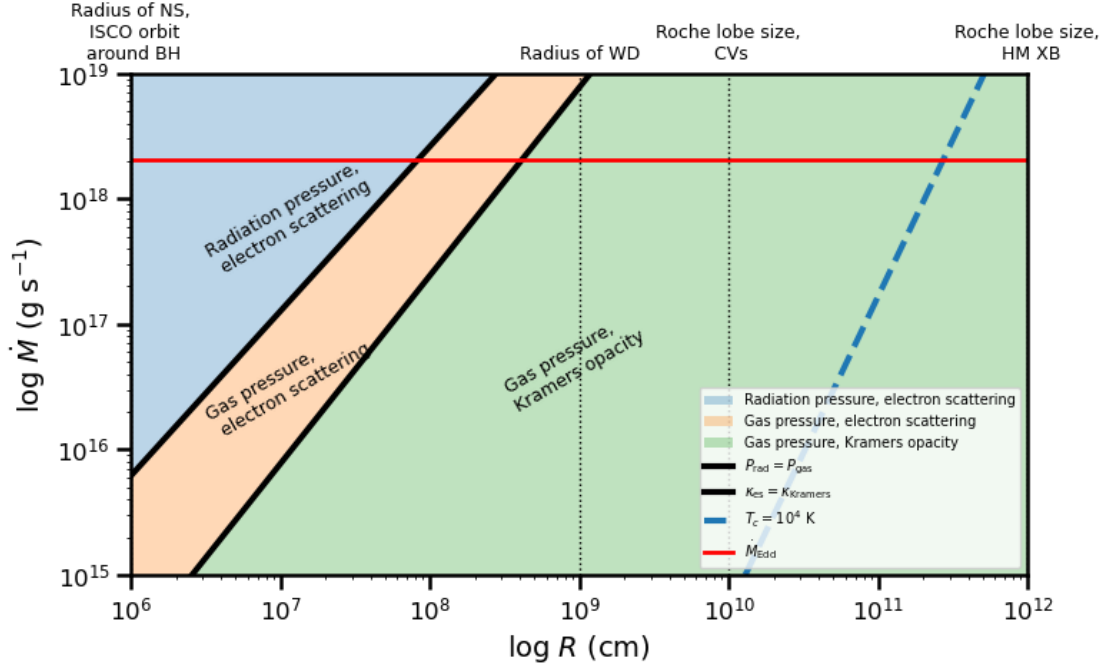


Figure 2: Regions of accretion disks dominated by different physical processes affecting thermal balance: pressure components, opacity sources. The disk outer radius must fit into the Roche lobe size, depending on the typical mass ratio of the binary. The inner radius can extend only to the ISCO orbit for BH, but cannot be smaller than WD radius for Cataclysmic Variables. The red solid line marks Eddington accretion rate limit. The blue dashed line marks region with temperature $10^4 K$ of Hydrogen recombination, where the other opacity sources are important.

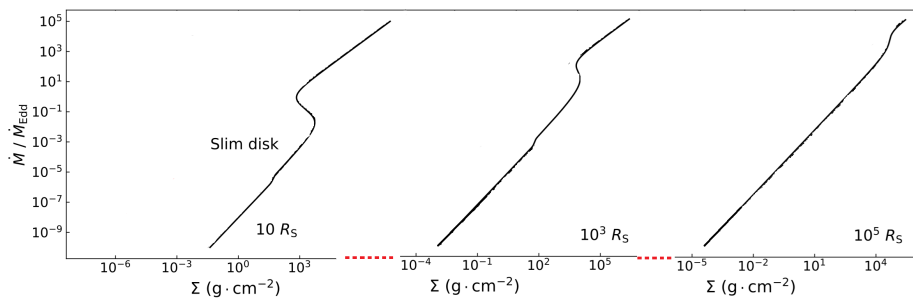


Figure 3: Symbolic representation of the thermal equilibria (S-curves) of the accretion disk. Since the curve apparently shifts up with radius, at high \dot{M} the instability might be driven by more distant, rather than inner, parts. However, the shape of the curve also varies with the radius, and at the largest radius showed above ($10^5 R_S$) the instability disappears, so the outermost part of the flow is always stable against RPI instability. Presented plots are based on the recent computations by [17].

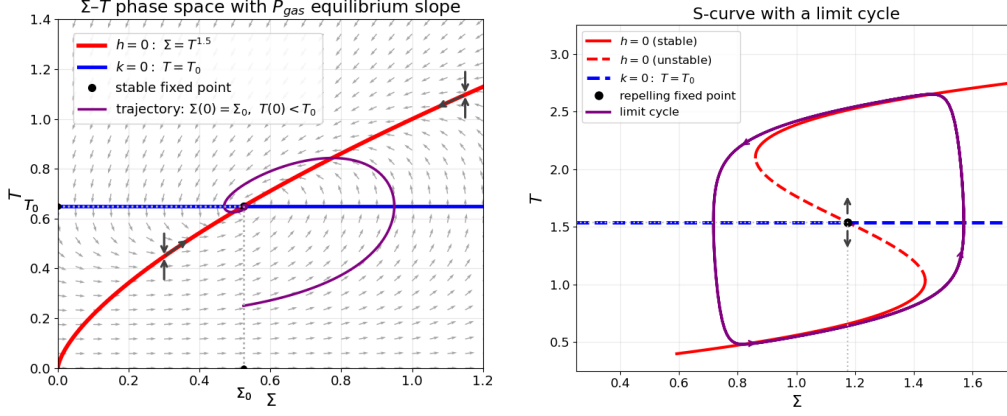


Figure 4: Attractor point on the stable branch of disk solutions (left) and limit cycle around repelling fixed point in the unstable branch of disk solutions (right).

advective cooling, are as follows:

$$Q_+ = \frac{3}{2}\alpha PH\Omega_K; \quad Q_- = \frac{4\sigma_B T^4}{3k\Sigma} + Q_{\text{adv}}; \quad Q_{\text{adv}} = -\frac{\dot{M}}{2\pi R^2} \frac{P}{\rho}$$

Here, P denotes the total (gas plus radiation) pressure, Ω_K is the Keplerian angular velocity at radius R , Σ is the disk surface density at this radius, H is the disk thickness, and T is its mid-plane temperature. The opacity is dominated by electron scattering, $\kappa = \kappa_{\text{es}}$. The local solutions form the S-curve [1], which for super-Eddington rate actually have a straight shape, as shown in Figure 3.

To analyze the stability of thermal equilibria, one may study small perturbations of density and temperature over time. In the equilibrium, the following vertically averaged balance is satisfied:

$$\frac{\partial T}{\partial t} = Q^+ - Q^- = h(T, \Sigma)$$

together with the diffusion equation for surface density:

$$\frac{\partial \Sigma}{\partial t} = (t_{\text{th}}/t_{\text{visc}})k(T, \Sigma)$$

where the timescales are defined as $t_{\text{visc}} = R^2/\nu$; $t_{\text{th}} = (\frac{v\phi}{c_s})^{-2}t_{\text{visc}}$, with ν being a kinematic viscosity, and c_s the speed of sound.

Nature of the stable and unstable fixed points (attractor and repeller) is visualized in Fig. 4. The solution is a fixed point that lies on the intersection of h and k curves, i.e. $Q^+ = Q^-$ and $T = T_0$ are satisfied simultaneously. On the stable branch of an S-curve, if $\partial\Sigma/\partial T > 0.$, the fixed point is attracting, i.e. any small perturbation of temperature is damped and the solution comes back to this fixed point. If the temperature rises slightly, the system moves along the $h = 0$ line, on the thermal timescale, before it finds the new value of Σ (that evolves on viscous timescale), searching for the new $k = 0$ intersection. But then the accretion rate will increase from local one \dot{M}_0 corresponding to the temperature $T = T_0$, so the local density will immediately drop. The temperature drops then accordingly, and the perturbation is damped.

A reverse situation is found at the unstable branch, with $\partial\Sigma/\partial T < 0$, where the fixed point is repelling. Here, any small perturbation of temperature leads to a runaway heating, with surface density decreasing on viscous timescale and accretion rate increasing above \dot{M}_0 . This thermal-viscous instability may be eventually controlled, if only another stable branch of equilibria is found. This stabilizing branch is the upper part of the S-curve. There again, a small perturbation in temperature, ie. its decrease, will lead to runaway cooling, as the local accretion rate will drop below \dot{M}_0 . As a result, for the accretion rates in the range corresponding to the negative slope of the S-curve, the disk annulus would oscillate between the lower and upper stable branches, and a type of limit-cycle oscillation is produced.

4. Numerical solutions

The local stationary solutions were discussed above, as resulting from the thermal heating and cooling balance. The closing equation which enable to find global structure of an accretion disk for a given accretion rate, and parameterized with viscosity α and black hole mass M , is:

$$F_{\text{tot}} = \frac{3GM\dot{M}}{8\pi R^3}$$

which gives the rate of locally dissipated heat due to gravitational potential energy of the black hole, and must be equal to the α disk viscous heating term. The model must also be supplemented with hydrostatic balance, of the form $c_s^2 = P_{\text{tot}}/\rho = H^2\Omega^2$ that relates speed of sound with rotation. Solving the set $Q_+ = Q_- = F_{\text{tot}}$ for temperature and density, at every radius, enables to find a global structure of the disk.

4.1 Global time dependent solutions

The 1D time dependent model proposed by [9] is solving the evolution of accretion disk subject to RPI. Governing equations, assuming Keplerian rotation, are viscous diffusion and energy transport, and they read:

$$\frac{\partial\Sigma}{\partial t} = \frac{1}{r} \frac{\partial}{\partial r} (3r^{1/2} \frac{\partial}{\partial r} (r^{1/2} v \Sigma))$$

and

$$\frac{\partial \ln T}{\partial t} + v_r \frac{\partial \ln T}{\partial r} = \left(\frac{4 - 3\beta}{12 - 10.5\beta} \right) \left(\frac{\partial \ln \Sigma}{\partial t} - \frac{\partial \ln H}{\partial t} + v_r \frac{\partial \ln \Sigma}{\partial r} \right) + \frac{Q_+ - Q_-}{(12 - 10.5\beta)PH}$$

where $\beta = P_{\text{gas}}/P_{\text{tot}}$ and coefficients in brackets can be derived from the ratio of specific heats, in the advection term see [23], [35], [15]. The changes over the thermal and viscous timescales produce long-term limit cycles oscillations., if the mass supply rate, \dot{M}_0 , is in the unstable regime. The extension of instability zone depends on global parameters, the viscosity α , and on the BH mass, as discussed in [12] - for supermassive BHs the zone is larger.

5. Observational evidence

There is a growing observational evidence for the RPI instability of accretion disks being in action in a wide range of astrophysical objects. Below we discuss several key examples, present preliminary results on the sources only recently discovered, and provide prospects for further studies.

5.1 Stellar mass black holes

The heartbeat oscillations were first found in GRS 1915+105 [3]. The source is presenting in some states large amplitude, quasi-periodic variability matching limit-cycle expectations. Timescales and luminosity swings of these flares are consistent with radiation-pressure-driven cycles, as shown in [9]. The source exhibits a variety of light variations, and heart-beat states showing repetitive bursts are only part of them. The apparent state of the source depends presumably on its past history (i.e. the hysteresis effect).

The other well established candidate is the microquasar IGR J17091, studied thoroughly in [2]. Its black hole mass $M = 6M_{\odot}$, spin $a = 0$, accretion rate $\dot{M} = 0.86 - 2.12 \times 10^{-8} M_{\odot} \text{ yr}^{-1}$, were found to be sufficient to explain the RPI-driven disk variability. The simulations performed by [13] using our 1-D hydro code GLADIS³ proved that limit cycle oscillations due to radiation pressure operate in the source, while the disk might be partially stabilized by wind outflow, as manifested in the spectral energy distributions with broad absorption features, that were weakened during the 'heartbeat' state intervals.

Further nonlinear diagnostics was made in [34] by means of the recurrence plots, and attractor reconstruction. The analysis proved evidence for low-dimensional deterministic structure, not pure noise, in the real data of a handful of X-ray sources, that were compared to the surrogate ones. The interpretation via RPI-driven limit cycles was made on the basis of the Recurrence Matix (RM), defined as:

$$\mathbf{R}_{i,j}(\epsilon) = \Theta(\epsilon - \|\vec{x}_i - \vec{x}_j\|), \quad i, j = 1, \dots, N,$$

where $\vec{x}_i = \vec{x}(t_i)$ is (N) points in phase space, reconstructed from time series as:

$$\vec{y}(t) = \{x(t), x(t + \Delta t), x(t + 2\Delta t), \dots, x(t + (m - 1)\Delta t)\}.$$

In this analysis, the significance of chaos is quantified by the Renyi entropy difference ($\ln K_2$) between the surrogate and real data. As a result, apart from the two canonical microquasars, GRS1915+105 and IGR17091, traces of non-linear dynamics were identified in: GX 339-4, XTE J1550-564 and GRO J1655-40.

5.2 Neutron stars

Neutron star SWIFT-J1858.6-0814 also shows limit-cycle oscillations [36]. This discovery gave the first observational evidence for shared instability between stellar mass black holes and neutron star systems. The multiwavelength observations hinted also on the effects of obscuration, radiation reprocessing and radio jet emission. Necessary condition to understand the source behavior is therefore its behaviour in other wavelengths.

To model the accretion instability in the neutron star case, we should consider effects of angular momentum transport around the rotating NS, whose hard surface is redistributing the viscously transported energy and decelerates the rotation of the accretion flow. As noted by [27], the radiation flux in the NS boundary layer (BL) is a substantial fraction of the Eddington limiting flux even for luminosities well below (~ 0.01 times) the Eddington luminosity. The BL layer rotates

³[github.org/agnieszkajaniuk/GLADIS](https://github.com/agnieszkajaniuk/GLADIS)

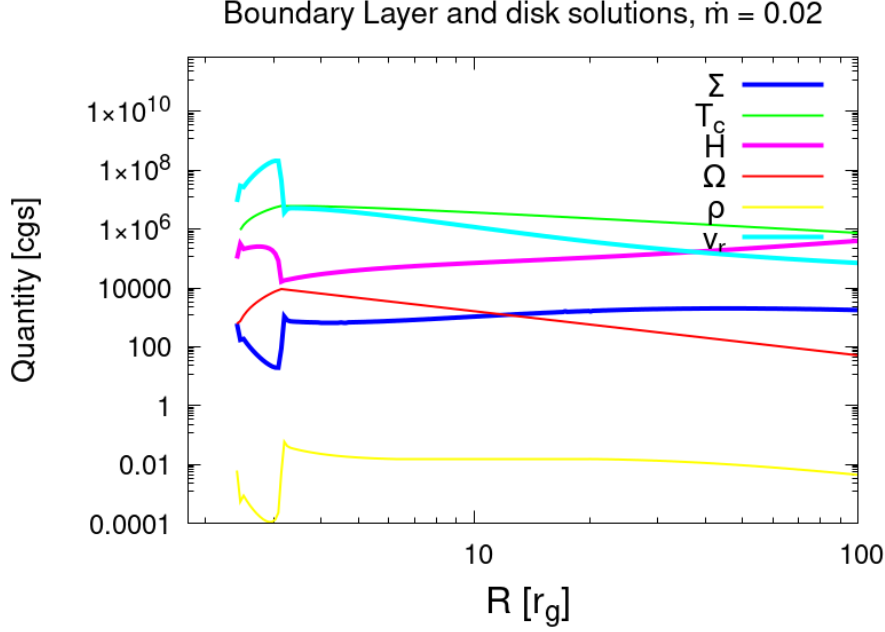


Figure 5: Solutions of the NS boundary layer structure, with a thin Keplerian accretion disk. Quantities plotted are: surface density, central temperature, geometrical thickness, angular velocity, density, and radial velocity. Parameters of the simulation: neutron star mass $M_{\text{NS}} = 1.4M_{\odot}$, neutron star radius $R_{\text{NS}} = 2.41 R_{\text{Schw}}$, angular momentum coupling parameter $j = 1.064$.

with sub-Keplerian velocity and is geometrically much thicker than the Keplerian disk surrounding it, hence the irradiation on the disk surface from the BL on the disk may be important,

To solve for the structure of BL, we follow the approach of [27] and modify the energy balance equations for accretion flow, that now is not assumed Keplerian. We solve for the $\Omega(R)$ profile, along with pressure, temperature and density gradients, with the following set of differential equations.

$$Q_+ - Q_- = 0 \quad (1)$$

where Q_- is the vertically averaged radiative cooling, and $Q_+ = Q_{\text{grav,kin}} - Q_{\text{trans}}$; with $Q_{\text{grav,kin}} = \frac{\dot{M}}{4\pi R} (\Omega_K^2 R + \Omega R^2 \frac{d\Omega}{dR} + \Omega^2 R)$ and $Q_{\text{trans}} = -\frac{\dot{M}}{4\pi R} \frac{d}{dR} (\Omega^2 R^2 - j\Omega\Omega_{\text{NS}}^K R_{\text{NS}}^2)$, standing for heating terms due to gravitational and kinetic energy losses in the BL, and for the divergence of the viscous energy transport rate, as explained in [27].

The angular momentum redistribution in the BL reads:

$$\frac{d\Omega}{dR} = \frac{v_r}{vR^2} (\Omega R^2 - j\Omega_{\text{NS}}^K R_{\text{NS}}^2) \quad (2)$$

and is parameterized by a constant j , that may be larger or smaller than 1.0.

The radial pressure gradient is solved from

$$v_r \frac{dv_r}{dR} + \frac{1}{\rho} \frac{dP}{dR} = (\Omega^2 - \Omega_K^2) R \quad (3)$$

The above three equations are solved together, but for simplicity only when $\Omega(R) < \Omega_K$. Otherwise, standard Keplerian disk solutions are solved. The resulting profiles of disk structure are shown in Fig. 5.

5.3 Irradiation of the disk by a central source

In a realistic situation, the accretion flow in the disk is surrounded by a hot medium, in a form of either a corona, or a spherical source. This medium may interact with the disk and influence the instability pattern in various ways. Dynamical interaction has been taken into account by [10] who introduced mass exchange between the disk and the hot corona, under the slab (i.e. 'sandwich-like') geometry. The hot corona above the disk had a virial temperature and varied in time according to the disk instability cycles. Observable consequences of this effect were manifested in time delays between hard and soft X-ray emission, and matched well with observations of GRS 1915+105.

We can also consider the effects of irradiation of the accretion disk from the central source with hard photons, under an arbitrary geometry. The formalism and equations were first introduced by [5] who modeled the CV type of instabilities and studied irradiated disks.

The temperature of the disk is changing due to additional heating from the central source, which is scaled with the local accretion rate and subject to geometrical effects.

$$T_c^4 = \frac{3}{8} \tau_{\text{tot}} T_{\text{eff}}^4 + T_{\text{irr}}^4 ; T_{\text{irr}}^4 = C \frac{\dot{M} c^2}{4\pi R^2} \quad (4)$$

In the above formula, the factor C includes the geometrical factor $\cos(\theta)$,

$$C = \eta(1 - \epsilon) \cos(\theta) \quad (5)$$

and η denotes the X-ray efficiency, while $1 - \epsilon$ shows the fraction of X-ray absorbed in the optically thick layers of the disk. In Figure 6 we present a sketch of the geometry sketch adopted in the new version of our GLADIS code (under development) which accounts for the disk irradiation by the central source. The geometrical factor $\cos(\theta)$ in Eq. 5 is defined as:

$$\cos(\theta) = \frac{\frac{dH_{\text{irr}}}{dR} - \frac{\Delta H_{\text{irr}}}{\Delta R}}{\sqrt{\left(1 + \left(\frac{\Delta H_{\text{irr}}}{\Delta R}\right)^2\right) \left(1 + \left(\frac{dH_{\text{irr}}}{dR}\right)^2\right)}} \quad (6)$$

where $\Delta H_{\text{irr}} = H - H_{\text{BL}}$, and $\Delta R = R - R_{\text{BL}}$ as marked in Fig. 6 and radial derivatives are computed during time dependent simulation, when the disk thickness is oscillating (note that it is slightly different from the prescription of [5]). Our goal is to model observations such as those shown in Fig. 7 where we present the lightcurve of 4U1630-47 as observed by NICER on 2023 March 27 (cf. [6]). A preliminary result from the new version of GLADIS is shown in Figure 8, where it is evident that the extra role of irradiation (red line) alters the regular accretion cycle which GLADIS calculates in its absence (blue line). The irradiation appears to introduce a faster cycle on top of the main one, due to its effect on the local instability/mass accretion rate.

5.4 Intermediate mass and supermassive BHs. Quasar duty cycles

RPI instability can reproduce the duration, period, and amplitude of the outbursts in the intermediate-mass black hole, HLX-1 [7] as well as it can be applied to the AGN phenomenology,

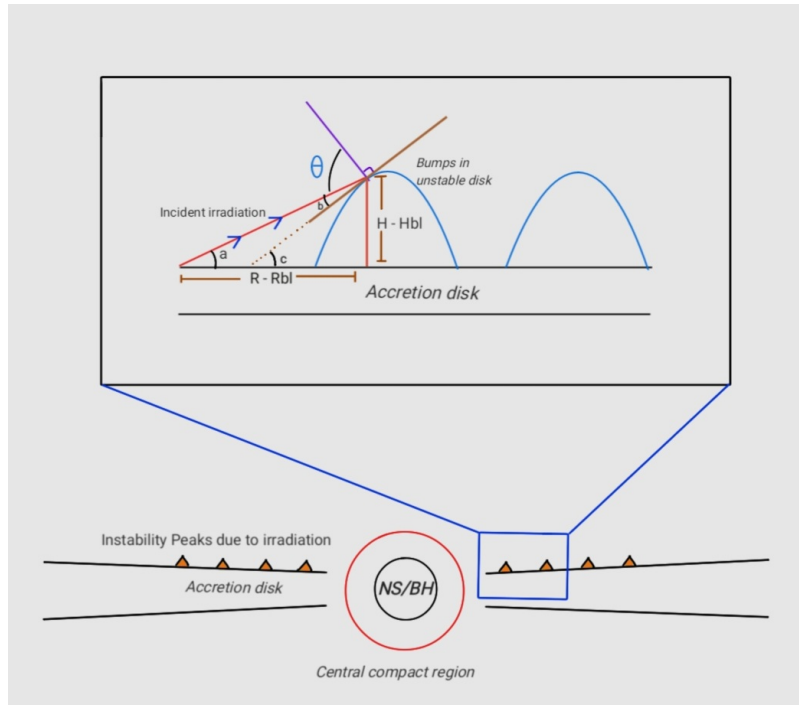


Figure 6: Artistic impression of a disk undergoing radiation pressure instability. In the top panel we show how the effect of irradiation from a central illuminating source (a compact corona or a boundary layer, at position R_{BL} , H_{BL}) will affect only the inner part of the instability waves. The effect of irradiation is proportional to the cosine of the angle θ between the incident ray and the normal to the surface of the disc.

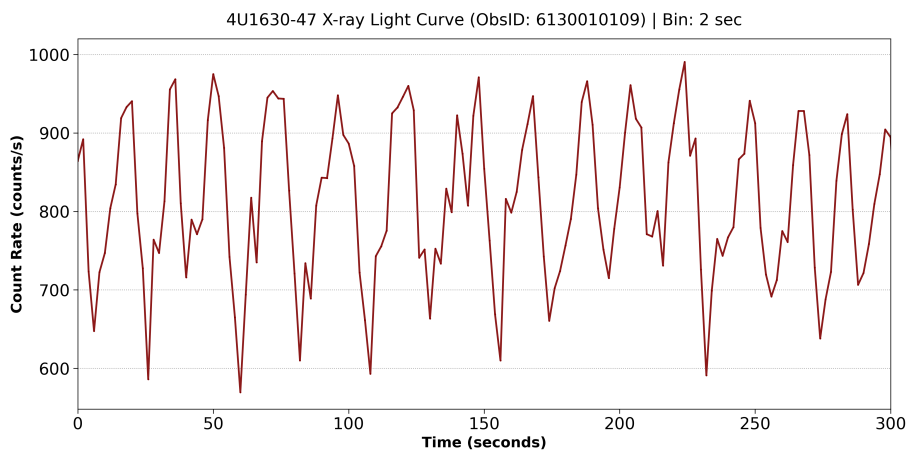


Figure 7: Lightcurve of the source 4U 1630-47, showing heartbeat states in NICER observation recorded on 2023 March 27 with obsID 6130010109. The lightcurve has been obtained using a binning interval of 2 seconds. The period of these oscillations are about 20-25 secs, cf. [6].

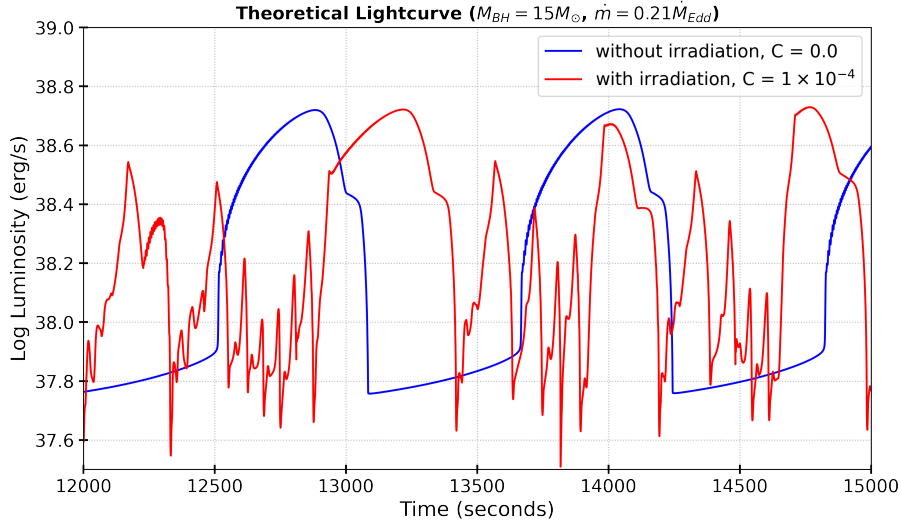


Figure 8: Theoretical lightcurves produced from GLADIS code including the effect of irradiation from the central compact region onto the disk around a black hole (red curve). For comparison, the non-irradiated disk evolution is shown (blue curve). The BH mass is $15 M_{\odot}$, accretion rate is $\dot{M} = 0.21 \dot{M}_{\text{Edd}}$, viscosity parameter is $\alpha = 0.01$.

as shown in [8], who investigated the importance of atomic processes at lower temperatures. With GLADIS code and a modified prescription of the viscous dissipation, the stabilizing effect of the iron opacity bump was examined and proven to be limited.

Quasars, in order to grow their central black hole masses should be active for 10^8 years. However, there are arguments that this growth is not steady but it has an intermittent character, with timescales of the individual episodes of $\sim 10^5$ years. The observational evidence is based on the size of the photo-ionized region in a typical quasar [29]. Another method to measure these timescales, giving similar results, is based on age estimates of the radio loud sources and uses the jet size (kinetic method) or estimate of the synchrotron cooling timescale [4]. Observations suggest also much more rapid changes in a given source, on timescales of years, stationary or propagating but they are most likely explained as re-collimation shocks [18].

Radiation pressure instabilities are expected to be present in AGN as the disks there are dominated by the radiation pressure. Models of such phenomenon [4, 7] imply the timescales of 100 to 10^5 years, depending on the black hole mass and accretion rate. However, the details depend essentially on the description of the viscosity, as discussed by [12] (see [7] for a more general treatment). Both the period, and particularly the outburst amplitude, are affected. There are also possible phenomena stabilizing the disk such as the presence of the warm corona, or winds. The statistical comparison of the models with the data is not simple as there are a number of mechanisms which should be included. Observational constraints on the ionized region can simply reflect the large density of the interstellar medium and too low jet or radiation power to expand further the ionized region, which then may not correspond to the source age.

Theoretical approach to determine whether RPI mechanism indeed works are rather difficult, so comparing simple models to the observational data seems a much more promising path. There were

attempts to explain the phenomenon of the rapid (timescales of a few years) changes in the AGN appearance in sources known as Changing-Look AGN (CL AGN) [32] but such short timescales in a roughly standard model can be only achieved in the case of a very small outer radius of the accretion disk [33]. This in turn can be only possible if the disk is formed in the tidal disruption event. Alternatively, since most of the CL AGN accrete at a few per cent Eddington rate [26], it may imply that the instability couples to the disruption of the inner flow, or is regulated by magnetic pressure, in a way which is not yet incorporated in the global modeling (see [25]).

6. Open Questions

State-of-the-art numerical simulations. Radiation-MHD simulations initiated by [22] and recently presented e.g. by [14] are the powerful tool that includes MRI transport, magnetic field evolution, vertical structure and radiation. Still, they resolve only local thermal timescales and due to limited duration cannot recover full long-term cycles. Technical challenges are met with the code's stiffness, and computations cost of radiation coupling. Magnetic pressure seems to be key factor that can modify or stabilize expected instability. The discrepancies between 1D long-term predictions and short-term multi-D outcomes reveal that local boxes can be thermally unstable, but other results show magnetically supported stability (see S. Hirose review in this Proceeding).

Also, although the local MHD simulation postulates the stabilizing influence of the atomic processes, only the global time-dependent model can reveal the global disk stability range estimation. This is due to the global diffusive nature of those processes.

Outlook and future directions. New observations with time-domain facilities, and multi-wavelength coordination are essential to obtain improved limit cycles and deterministic chaos metrics in wide class of astrophysical sources with accreting compact stars. Theoretical advances should encompass: longer duration and multi D simulations, reduced-order informed models, and coupling to other parts of accretion flows, such as boundary layers, coronas, winds and jets. Cross-disciplinary tools that may help the advancements in the field are powerful Machine Learning tools for pattern recognition, and studies of other dynamical systems for better interpretation.

Acknowledgments We thank Lukasz Klepczarek for technical support and discussions. We acknowledge Poland's high-performance Infrastructure PLGrid through HPC Centers: ACK Cyfronet AGH for providing computer facilities and support within computational grant no. PLG/2025/018232 and Warsaw ICM within grant GCT under allocation g101-2281. This work was supported by the Polish National Science Center grant 2023/50/A/ST9/00527.

References

- [1] M.A. Abramowicz, B. Czerny, J.P. Lasota, E. Szuszkiewicz, *Slim Accretion Disks*, *ApJ* **332**, 646 (1988)
- [2] D. Altamirano, T. Belloni, M. Linares, et al., *The Faint "Heartbeats" of IGR J17091-3624: An Exceptional Black Hole Candidate*, *ApJL* **742** 17 (2011)
- [3] T. Belloni, M. Klein-Wolt, M. Mendez, et al. *A model-independent analysis of the variability of GRS 1915+105*, *A&A* **355** 271 (2000)

- [4] B. Czerny, A. Siemiginowska, A. Janiuk, et al., *Accretion Disk Model of Short-Timescale Intermittent Activity in Young Radio Sources*, *ApJ* **698** 840 (2009)
- [5] Dubus G., et al., *X-ray irradiation in low-mass binary systems*, *MNRAS* **303** 139 (1999)
- [6] Fan N., et al., *NICER Spectral and Timing Analysis of 4U 1630-47 and Its Heartbeat State*, *ApJ* **984** 31
- [7] M. Grzedzielski, A., Janiuk, B. Czerny, Q. Wu, *Modified viscosity in accretion disks. Application to Galactic black hole binaries, intermediate mass black holes, and active galactic nuclei* *A&A* **603** 110 (2017a)
- [8] M. Grzedzielski, A., Janiuk, B. Czerny, *Local Stability and Global Instability in Iron-opaque Disks* *ApJ* **845** 20 (2017b)
- [9] A. Janiuk, B. Czerny, A. Siemiginowska, *Radiation Pressure Instability Driven Variability in the Accreting Black Holes*, *ApJ*, **576** 908 (2002)
- [10] A. Janiuk, B. Czerny, *Time-delays between the soft and hard X-ray bands in GRS 1915+105*, *MNRAS* **356** 205 (2005)
- [11] A. Janiuk, B. Czerny, *Accreting corona model of the X-ray variability in soft state X-ray binaries and active galactic nuclei*, *A&A* **466** 793 (2007)
- [12] A. Janiuk, B. Czerny, *On different types of instabilities in black hole accretion discs: implications for X-ray binaries and active galactic nuclei*, *MNRAS*, **414** 2186 (2011)
- [13] A. Janiuk, M. Grzedzielski, F. Capitanio, S. Bianchi, *Interplay between heartbeat oscillations and wind outflow in microquasar IGR J17091-3624*, *A&A* **574** 92 (2015)
- [14] Y.F. Jiang, et al., *Global Radiation Magnetohydrodynamic Simulations of sub-Eddington Accretion Disks around Supermassive Black Holes*, *ApJ* **885** 144 (2019)
- [15] J.P. Lasota, D. Pelat, *Variability of accretion discs around compact objects*, *A&A* **249** 574 (1991)
- [16] A.P. Lightman, D.M. Eardley, *Black Holes in Binary Systems: Instability of Disk Accretion*, *ApJ* **187** L1 (1974)
- [17] M. Liu et al., *A generalized solution for advection-dominated accretion flow, standard disc, and slim disc*, *MNRAS* **539** 69 (2025)
- [18] M.L. Lister, et al. *MOJAVE: Monitoring of Jets in Active Galactic Nuclei with VLBA Experiments. VI. Kinematics Analysis of a Complete Sample of Blazar Jets*, *AJ* **138** 1874 (2009) *MNRAS*, **292** 679 (1997)
- [19] D. Lynden-Bell, J. E. Pringle, *The Evolution of Viscous Discs and the Origin of the Nebular Variables*, *MNRAS* **168** 603 (1974)

- [20] I. Novikov, K. Thorne, *Astrophysics of Black Holes*, In: *Black Holes (Les Astres Occlus)*, eds. C. DeWitt & B. S. DeWitt, Gordon and Breach, New York **343–450** (1973)
- [21] F. Meyer & E. Meyer-Hofmeister *On the Elusive Cause of Cataclysmic Variable Outbursts*, *A & A* **104** L10–L12 (1981)
- [22] K. Ohsuga, S. Mineshige *Global Structure of Three Distinct Accretion Flows and Outflows around Black Holes from Two-dimensional Radiation-magnetohydrodynamic Simulations*, *ApJ* **736** 18 (2011)
- [23] B. Paczynski, G. Bisnovaty-Kogan *A Model of a Thin Accretion Disk around a Black Hole*, *Acta Astron.* **31** 283 (1981)
- [24] B. Paczynski, P.J. Wiita, *Thick accretion disks and supercritical luminosities*, *A&A* **88** 23 (1980)
- [25] X. Pan, S.L. Li, X. Cao, et al., *A Disk Instability Model for the Quasi-periodic Eruptions of GSN 069*, *ApJL* **928** 18 (2022)
- [26] S. Panda, M. Sniegowska, *Changing-look Active Galactic Nuclei. I. Tracking the Transition on the Main Sequence of Quasars*, *ApJ* **272** 13 (2024)
- [27] R. Popham, R. Sunyaev, *Accretion Disk Boundary Layers around Neutron Stars: X-Ray Production in Low-Mass X-Ray Binaries*, *ApJ* **547** 355 (2001)
- [28] N.I. Shakura, R.A. Sunyaev, *Black holes in binary systems. Observational appearance.*, *A&A* **24** 337 (1973)
- [29] K. Schawinski, et al., *Active galactic nuclei flicker: an observational estimate of the duration of black hole growth phases of $\sim 10^5$ yr*, *MNRAS* **451** 2517 (2015)
- [30] S.L. Shapiro, A.P. Lightman, & D.M. Eardley, *A two-temperature accretion disk model for Cygnus X-1 – Structure and spectrum*, *ApJ* **204** 187 (1976)
- [31] J. Smak, *Accretion in cataclysmic binaries. IV. Accretion disks in dwarf novae.*, *Acta Astron.* **34** 161 (1984)
- [32] M. Sniegowska, et al., *Possible mechanism for multiple changing-look phenomena in active galactic nuclei*, *A&A*, **641** 167 (2020)
- [33] M. Sniegowska, et al., *Modified models of radiation pressure instability applied to 10 , 10^5 , and $10^7 M_{\odot}$ accreting black holes*, *A&A* **672** 19 (2023)
- [34] P. Sukova, A. Janiuk, M. Grzedzielski, *Chaotic and stochastic processes in the accretion flows of the black hole X-ray binaries revealed by recurrence analysis*, *A&A* **586** 143 (2016)
- [35] R.E. Taam, Lin, *The evolution of the inner regions of viscous accretion disks surrounding neutron stars*, *ApJ* **287** 761 (1984)

- [36] F.M. Vincentelli, J. Neilsen, B. Tetarenko, et al., *A shared accretion instability for black holes and neutron stars*, *Nature*, **615** 7950 (2023)
- [37] Q. Wu, B. Czerny, M. Grzedzielski, et al., *The Universal “Heartbeat” Oscillations in Black Hole Systems Across the Mass-scale*, *ApJ* **833** 79 (2016)